

# Estimating sensible heat flux using surface renewal analysis and the flux variance method: A case study over olive trees at Sástago (NE of Spain)

F. Castellvi

Departamento Medi Ambient i Ciències del Sòl, Escola Tècnica Superior d'Enginyeria Agrària, Lleida, Spain

A. Martínez-Cob

Departamento Genética y Producción Vegetal (Estación Experimental de Aula Dei), LAAMA (DGA-CSIC), Zaragoza, Spain

Received 14 February 2005; revised 25 May 2005; accepted 14 June 2005; published 27 September 2005.

[1] The eddy covariance technique for measuring surface fluxes is often not affordable outside experimental research institutes. Therefore knowledge of the performance of alternative methods for determining surface fluxes is valuable. The performance of surface renewal (SR) analysis and the flux variance (FV) method for estimating sensible heat flux has been evaluated in an experiment carried out over a heterogeneous canopy (olive orchard, 50% ground cover) at a semiarid climate in a windy area. Measurements were made at a single level close to the canopy top. SR analysis was accurate under both stable and unstable conditions. The FV method also showed a good performance under unstable conditions, but it was uncertain near neutral conditions and was not applicable under stable conditions.

**Citation:** Castellvi, F., and A. Martínez-Cob (2005), Estimating sensible heat flux using surface renewal analysis and the flux variance method: A case study over olive trees at Sástago (NE of Spain), *Water Resour. Res.*, 41, W09422, doi:10.1029/2005WR004035.

## 1. Introduction

[2] A campaign for estimating sensible heat flux over a drip irrigated olive orchard in a semiarid area has been carried out. The experiment was conducted in a region where agriculture plays a key role for the economy and an accurate management of the available water resources is crucial. Accurate weighing lysimeters and the eddy covariance technique for measuring surface fluxes are often not affordable outside experimental research institutes. Therefore there is a need to analyze the performance of alternative methods for determining surface fluxes. On the basis of the surface energy balance equation, knowledge of sensible heat flux obtained from inexpensive and robust sensors is crucial for estimating latent heat flux since measurement of the available net surface energy is actually affordable. The aim of this paper is therefore the evaluation of two methods for estimating sensible heat flux over such a heterogeneous canopy. For practical reasons, to avoid the need to set up tall micrometeorological towers and to use the minimum number of robust sensors, in order to minimize costs and maintenance that permits a denser spatial cover, it was assumed that measurements are only available at a single level close to the canopy top. The performance of the following two methods was tested.

[3] 1. One method was surface renewal (SR) analysis in conjunction with air temperature traces [Paw U *et al.*, 1995] (equation (1)), using a recent expression for estimating

parameter  $\alpha$  proposed by Castellvi [2004]. SR analysis for estimating sensible heat flux over vegetated surfaces was selected because it has been proved to perform well over a variety of canopies, though most studies have been carried out under unstable conditions and over homogeneous canopies [Paw U *et al.*, 1995; Katul *et al.*, 1996; Snyder *et al.*, 1996; Chen *et al.*, 1997a, 1997b; Spano *et al.*, 1997, 2000; Zapata and Martínez-Cob, 2001; Castellvi *et al.*, 2002; Castellvi, 2004].

[4] 2. The second is the flux variance (FV) method because it has been extensively proved and recommended when the eddy covariance method is not affordable. Though the flux variance method has been mainly analyzed under unstable conditions and operating in the inertial sublayer, good performance was also found in some experiments when operating in the roughness sublayer over homogeneous canopies [Weaver, 1990; Lloyd *et al.*, 1991; Padro, 1993; De Bruin *et al.*, 1993; Albertson *et al.*, 1995; Katul *et al.*, 1995, 1996; Hsieh and Katul, 1996; Wesson *et al.*, 2001].

[5] In our experiment, the bases on which SR analysis and the FV method are build were not completely met (see section 2). Nevertheless, reasonable sensible heat flux estimates may still be useful for some field applications. For instance, determination of accurate irrigation crop water requirements is desired for irrigation scheduling and design. However, so many other factors are involved (crop varieties, cycles and management, soil characteristics, water availability, irrigation system design, wind conditions during sprinkler irrigation, pressure in water delivery systems, age of irrigation systems, and so on) that such highly accurate crop water requirements

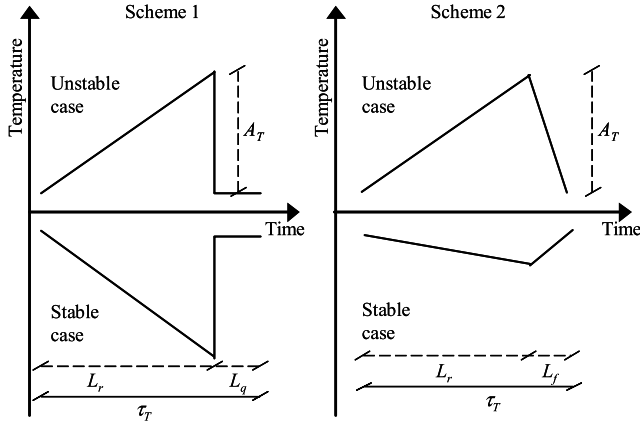


**Figure 1.** Surface renewal analysis ramp models: (left) scheme 1, assuming a sharp instantaneous drop in air temperature, and (right) scheme 2, assuming a finite microfront.  $L_r$ ,  $L_q$ , and  $L_f$  are the warming, quiescent, and microfront periods, respectively.  $A_T$  is the ramp amplitude, and  $\tau_T$  is the total ramp duration.

may not always be accomplished. In such situations, estimates of latent heat flux, obtained through a surface energy balance from reasonable sensible heat flux estimates are useful.

## 2. Theory

### 2.1. Surface Renewal Analysis

[6] SR analysis assumes that turbulent exchange on any scalar is driven by the regular replacement of the air parcel in contact with the surface where exchange occurs. An air parcel sweeps down to the surface and replaces another that ejects from the canopy once the latter has enriched or depleted the scalar. This process appears as ramp-like time series when high-frequency measurements of the scalar are plotted versus time. An ideal and comprehensive scheme for this process was originally presented by *Paw U et al.* [1995] (scheme 1, Figure 1) and *Chen et al.* [1997a] (scheme 2, Figure 1). Sensible heat flux density from the surface at height  $z$  (within the canopy, the roughness or the inertial sublayers) is determined by the following expression [*Paw U et al.*, 1995; *Snyder et al.*, 1996; *Chen et al.*, 1997a]:

$$H = (\alpha z) \rho C_p \frac{A_T}{\tau_T} \quad (1)$$

where  $\rho$  and  $C_p$  are the density and specific heat of air at constant pressure, respectively;  $A_T$  and  $\tau_T$  are the mean ramp amplitude and the inverse ramp frequency of the air temperature trace over the averaging period (commonly half hour), respectively. Methods for determining ramp dimensions can be found in the works of *Paw U et al.* [1995], *Katul et al.* [1996], *Snyder et al.* [1996], and *Paw U et al.* [2002] for the ramp model of scheme 1 (Figure 1) and in the work of *Chen et al.* [1997a] for the ramp model of scheme 2 (Figure 1). Ramp parameters of scheme 2 require measurements of the scalar at very high

frequencies because the sampling must be lower than the microfront time period. A practical approach for estimating ramp dimensions according to scheme 2, useful for field applications, is described in Appendix A based on the work by *Chen et al.* [1997b].

[7] The variable  $(\alpha z)$  is the volume of air, with height  $z$ , per unit ground area exchanged on average for each ramp in the sample period [*Paw U et al.*, 1995]. Equation (1), based on the energy conservation equation, assumes that advection is negligible and parameter  $\alpha$  requires calibration. During the last decade, several studies have analyzed the SR method giving valuable understanding of the performance of parameter  $\alpha$  [*Castellvi*, 2004, and references therein]. Calibration of parameter  $\alpha$  can be avoided when the canopy is divided into sublayers. For thin sublayers, it may be assumed  $\alpha \approx 1$  [*Paw U et al.*, 1995] and the total flux density can be estimated as the sum of equation (1) applied for different sublayers [*Spano et al.*, 2000]. However, this requires measuring the traces of the scalar at various heights within the canopy. *Castellvi et al.* [2002] interpreted the variable  $(\alpha z)$  as the mean eddy size responsible for the renewal process. On the basis of the understanding that temperature ramps in traces represent injections of sensible heat flux into the atmosphere that changes the local vertical gradient of temperature, *Castellvi* [2004] derived the following relationship for estimating the parameter  $\alpha$  when measuring above the canopy.

$$\alpha = \begin{cases} \left[ \frac{k(z-d)\tau_T u_*}{\pi z^2 \phi_h(\zeta)} \right]^{1/2} & z > z^* \\ \left[ \frac{k z^* \tau_T u_*}{\pi z^2 \phi_h(\zeta)} \right]^{1/2} & h \leq z \leq z^* \end{cases} \quad (2)$$

where  $d$  is the zero-plane displacement;  $z^*$  is the roughness sublayer depth;  $h$  is the canopy height;  $u_*$  is the friction velocity;  $\zeta$  is a stability parameter defined as  $(z-d)/L_0$ , with  $L_0$  being the Obukov length,  $\phi_h(\zeta)$  is the stability function for heat transfer valid in the inertial sublayer that is described below in equation (4), and  $k \sim 0.35$  is the Von Kármán constant which is in according to equation (4). Equation (2) is based on the one-dimensional diffusion equation and, following *Cellier and Brunet* [1992], it assumes that the stability function for heat valid in the roughness sublayer is  $(z-d)/z^* \phi_h(\zeta)$ . The Obukov length is defined as [*Brutsaert*, 1988]:

$$L_0 = - \frac{u_*^3 \rho}{kg \left( \frac{H}{\rho C_p} + 0.61E \right)} \approx - \frac{u_*^3 T}{kg \left( \frac{H}{\rho C_p} \right)} \quad (3)$$

where  $T$  is the mean absolute air temperature,  $E$  is the water vapor flux (traditionally omitted for dry climates) and  $g$  is the acceleration due to gravity. Equation (3) can be approximated to the right-hand expression when water vapor flux is small. A widely accepted formulation for  $\phi_h(\zeta)$  (also valid for any flux scalar) is the following [*Businger et al.*, 1971]:

$$\phi_h(\zeta) = \begin{cases} 0.74/\sqrt{1-9\zeta} & \zeta < 0 \\ 0.74 & \zeta = 0 \\ 0.74 + 5\zeta & \zeta > 0 \end{cases} \quad (4)$$

[8] Thus, combining equations (1), (2), (3) and (A5), *Castellvi* [2004] proposed the following expression for estimating sensible heat flux:

$$H = \begin{cases} \rho C_p \left(\frac{g}{T}\right)^{1/5} \frac{[k(z-d)^{4/5}]}{\pi^{3/5}} \left[-\gamma^3 \frac{S_{(rx)}^3}{r_x}\right]^{3/5} \frac{1}{A_T^{3/5}} \left[\frac{1}{-\zeta \phi_h^3(\zeta)}\right]^{1/5} & z > z^* \\ \rho C_p \left(\frac{g}{T}\right)^{1/5} k^{4/5} \left(\frac{z^*}{\pi}\right)^{3/5} z^{1/5} \left[-\gamma^3 \frac{S_{(rx)}^3}{r_x}\right]^{3/5} \frac{1}{A_T^{3/5}} \left[\frac{1}{-\zeta \phi_h^3(\zeta)}\right]^{1/5} & h \leq z \leq z^* \end{cases} \quad (5)$$

where  $S_{(rx)}^3$ ,  $r_x$  and  $\gamma$  are, respectively, the third order of the structure function for temperature, the time lag and a rather conservative parameter, all of which are defined in Appendix A. Because equation (5) depends on the stability parameter, wind speed measurements are also required as input. According to equation (4), the free convection limit for equation (5) holds for  $\zeta \leq -0.03$  with a relative error of less than 8.5% and can be expressed as [*Castellvi*, 2004]:

$$H = \begin{cases} 2.4 \rho C_p \left(\frac{g}{T}\right)^{1/5} \frac{[k(z-d)^{4/5}]}{\pi^{3/5}} \left[-\gamma^3 \frac{S_{(rx)}^3}{r_x}\right]^{3/5} \frac{1}{A_T^{3/5}} & z > z^* \\ 2.4 \rho C_p \left(\frac{g}{T}\right)^{1/5} k^{4/5} \left(\frac{z^*}{\pi}\right)^{3/5} z^{1/5} \left[-\gamma^3 \frac{S_{(rx)}^3}{r_x}\right]^{3/5} \frac{1}{A_T^{3/5}} & h \leq z \leq z^* \end{cases} \quad (6)$$

[9] For a variety of short canopies, equations (5) and (6) with a parameter  $\gamma = 1.1$  (Table A1) performed well using measurements taken at different heights above the canopy. Therefore equations (5) and (6) could be considered, in practice, exempt from calibration [*Castellvi*, 2004]. Despite equations (1) and (2) do not have to be valid when measuring above but close to a heterogeneous canopy, *Castellvi* [2004] showed a case over grapevines (60% ground cover) where equations (1) and (2) provided a good performance.

## 2.2. Flux Variance Method

[10] The FV method [*Tillman*, 1972] is based on Monin-Obukhov similarity theory (MOST). It is a well-established method that has been the subject of intensive research over the last three decades, though mainly under unstable conditions and for estimating sensible heat flux. Its good performance has been extensively proved and recommended when eddy covariance system is not affordable [*Wesely*, 1988; *Kader and Yaglom*, 1990; *Weaver*, 1990; *Lloyd et al.*, 1991; *Padro*, 1993; *Albertson et al.*, 1995; *Katul et al.*, 1995, 1996; *Hsieh and Katul*, 1996; *Wesson et al.*, 2001]. For estimating sensible heat flux, *Tillman* [1972] proposed:

$$H = \begin{cases} \rho C_p \left(\frac{\sigma_T}{C_1}\right)^{3/2} \left[\frac{kg(z-d)}{T}\right]^{1/2} \left(\frac{0.05 - \zeta}{-\zeta}\right)^{1/2} & \zeta < 0 \\ -\rho C_p \left(\frac{\sigma_T}{C_2}\right)^{3/2} \left[\frac{kg(z-d)}{T}\right]^{1/2} \frac{1}{\zeta} & \zeta \geq 0 \end{cases} \quad (7)$$

where  $\sigma_T$  is the air temperature standard deviation measured at high frequency. The free convection limit approach for

equation (7) has proven to operate under slightly unstable conditions and can be expressed as

$$H = \rho C_p \left(\frac{\sigma_T}{C_1}\right)^{3/2} \left[\frac{kg(z-d)}{T}\right]^{1/2} \quad \zeta \leq -0.04 \quad (8)$$

[11] Equations (7) and (8) can be obtained combining equation (3), the generalized expression for sensible heat flux ( $H = \rho C_p u_* T_*$ , where  $T_*$  is the surface temperature scale) and the similarity function,  $g(\zeta)$ , that involves  $\sigma_T$  and  $T_*$  as follows:

$$g(\zeta) = \frac{T_*}{\sigma_T} = \begin{cases} (C_0 - \zeta)^{1/3} / C_1 & \zeta < 0 \\ 1 / C_2 & \zeta \geq 0 \end{cases} \quad (9)$$

where  $C_0$ ,  $C_1$  and  $C_2$  are similarity constants that can be set to 0.05, 0.95 and  $-2.0$ , respectively [*Tillman*, 1972; *Stull*, 1991]. However,  $C_2$  is an ill-defined constant. Several studies have shown that it ranges from 1.8 to 3 and that site-specific calibration is recommended [*Stull*, 1991; *De Bruin et al.*, 1993; *Wesson et al.*, 2001; *Pahlow et al.*, 2001]. For stable atmospheric conditions, *Pahlow et al.* [2001] proposed continuity in equation (9), and their experimental data showed that  $g(\zeta)$  rapid converges to  $C_2$  for  $\zeta > 0.0015$  and resulted very uncertain within the interval  $0 \leq \zeta \leq 0.0015$ . In terms of input data requirements, equations (5) and (6) are directly comparable to equations (7) and (8), respectively.

[12] MOST refers to the surface layer over an extensive flat and homogenous terrain. In practice this situation is difficult to find. Then, though equations (7), (8) and (9) do not need to be valid in other field conditions, the performance, robustness or applicability of the FV method has also been investigated over surfaces that are far of being ideal including nonuniform terrain, advective conditions and measurements taken close to the canopy [*Weaver*, 1990; *De Bruin et al.*, 1991; *Katul et al.*, 1996; *Wesson et al.*, 2001, sect. 5].

## 3. Materials and Method

### 3.1. Site Description and Experimental Setup

[13] The campaign was carried out from 15 April to 26 July 2004 (days of the year 106 to 208) over a 7 years old commercial olive orchard located at Sástago (Zaragoza) in the river Ebro basin (NE of Spain,  $41^\circ 18' 04''$ N latitude,  $0^\circ 21' 51''$ W longitude, 150 m elevation above sea level). The area is windy and dry. The most frequent wind direction is northwest (along the basin axis). Drip irrigation was applied each day using preinstalled emitters at 1 m spacing and a discharge of 3.8 L/Ha. The canopy top was 3.4 m tall. Trees were planted at a spacing of 6.0 m  $\times$  3.5 m, approximately. The soil canopy cover was 50%, approximately. Surface area of the orchard was about 64 Ha and a micrometeorological tower (6.0 m height) supporting different sensors was located at about 250 m, 650 m, 400 m and 320 m from the south, north, west and east edges of the plot, respec-



tively. Two dataloggers (Campbell CR23X and CR10X) were used to record the micrometeorological data.

### 3.1.1. CR23X

[14] A 3-D sonic anemometer (Campbell CSAT3) operating at 10 Hz was used to record 30-min averages, standard deviations and the respective covariances, of the three-component wind velocities and the sonic temperature. The CSAT3 was set at 4.9 m above soil surface and facing toward NW. Likewise, a net radiometer (Q-7, Radiation and Energy Balance Systems) and a soil temperature probe (Campbell TCAV probe) operating at 0.05 Hz were used to record 30-min averages of net radiation and soil temperature. The net radiometer was installed at the same height above the soil as the CSAT3. The soil temperature probes were buried at 0.02–0.06 m depths, one between adjacent rows and the other between trees within the same row.

### 3.1.2. CR10X

[15] Two fine wire thermocouples (76  $\mu\text{m}$  diameter, Campbell Scientific, TCB-3) operating at 4 Hz were used to record 30-min averages and standard deviation of air temperature and the 10-min sums of the second, third, and fifth moments of the differences between high-frequency air temperature for two time lags, 0.25 and 0.75 s. During postprocessing, 30-min sums were obtained from the 10-min ones and the corresponding second-, third-, and fifth-order structure functions were obtained applying equation (A1). This procedure was done to avoid getting 30-min sums of the second, third, and fifth moments of temperature differences above  $\pm 99999$  which is the maximum value that a CR10 datalogger can store. These two fine wire thermocouples were set at 5.1 and 3.5 m above soil surface. Likewise, a HMP45AC (Vaisala) probe and four soil heat flux plates (Hukseflux HFP01) operating at 0.05 Hz were used to record 30-min averages of air temperature and relative humidity, and soil heat flux, respectively. The HMP45AC probe was installed at 4.1 m above soil surface. Soil heat flux plates were buried at 0.08 m depth, at the same spots as the TCAV probe. The recorded soil heat flux values were corrected as described by Allen *et al.* [1996] using the soil temperature records to get soil heat flux at soil surface. At each 30-min period, the four soil heat flux values thus obtained were averaged.

[16] A gap from days 188 to 190 (6–8 July) in the data set was due to power malfunction. Other minor gaps were due to farmer practices, maintenance of the equipment and rainy periods. A set of 3793 half-hour samples (1886 under stable and 1907 under unstable conditions) was thus obtained.

## 3.2. Method

[17] It was assumed that measurements are available at one height above but close to the canopy top. Therefore friction velocity cannot be determined using traditional procedures based on the wind profile [Brutsaert, 1988], and the following procedure was used for determining sensible heat flux. The actual friction velocity was estimated through the horizontal wind speed standard deviation,  $\sigma_u$ , and the mean horizontal wind speed,  $u$ , as follows [Kaimal and Finnigan, 1994]:

$$u_* = a_1 \sigma_u \quad (10a)$$

$$u_* = a_2 u \quad (10b)$$

[18] Wind profile was not available; hence the zero plane displacement in equations (7) and (8) was assumed negligible as the canopy was open, without understories and the crown was not dense. The stability parameter was determined solving equation (3) after implementing equations (10a) or (10b) for friction velocity and the corresponding expression for sensible heat flux, equations (5) or (7) for SR analysis or the FV method, respectively. Simulated annealing procedure [Goffe *et al.*, 1994] was used for optimizing the stability parameter. The optimization process requires bounds for the stability parameter and selection of the expression for  $\phi_h(\zeta)$ , equation (4). This requires previous knowledge of the atmospheric surface layer stability condition to start the process. The sign of the ramp amplitude (Figure 1) can be used for distinguishing stable and unstable conditions. This method is straightforward because the stability parameter and the third-order temperature structure function (see equation (A5)) have the same sign and avoids the need of extra measurements. As a rule of thumb, the roughness sublayer depth in equation (5) was set to  $z^* = 12$  m. Following Cellier and Brunet [1992], it was estimated as 3.5 times the frontal stream-wise mean interrow space (3.5 m). The parameter  $\gamma$  was set to 1.0 (Table A1). Simulated annealing is a global optimization method that distinguishes between different local optima. Starting from an initial point, the algorithm takes a step and the function is evaluated. When minimizing a function, any downhill step is accepted and the process repeated from this new point. However, an uphill step may be accepted. Thus it can escape from local optima. This uphill decision is made by the Metropolis criteria [Metropolis *et al.*, 1953; Press *et al.*, 1992]. As the optimization process proceeds, the length of the steps decline and the algorithm closes in on the global optimum. Since the algorithm makes very few assumptions regarding the function to be optimized, simulated annealing is recommended as a local optimizer for difficult functions. Goffe *et al.* [1994] showed this procedure be superior to multiple restarts of conventional optimization routines for difficult optimization problems.

[19] Summarizing, the following set of sensible heat flux estimates were determined: (1) eddy covariance ( $H_{EC}$ ),  $H_{EC} = \rho C_p \overline{w'T'}$ , where  $\overline{w'T'}$  is the covariance between the fluctuations of vertical wind speed and sonic temperature; (2) SR analysis with equations (5) and (6) (free convection limit) at 5.1 m ( $H_{SR-UP}$  and  $H_{SR-FL-UP}$ , respectively) and 3.4 m ( $H_{SR-LOW}$  and  $H_{SR-FL-LOW}$ , respectively) above soil surface; and (3) sensible heat flux using the FV method with equations (7) and (8) (free convection limit) at 5.1 m ( $H_{VA-UP}$  and  $H_{VA-FL-UP}$ , respectively) and 3.4 m ( $H_{VA-LOW}$  and  $H_{VA-FL-LOW}$ , respectively) above soil surface.

## 4. Results and Discussion

[20] The sign of the ramp amplitude was used for distinguishing the stable and unstable conditions for each sample to start the optimization process. This procedure identified a set of 259 samples that were not in accordance with the sign of the sensible heat flux measured with the sonic anemometer. This set includes the mistakes made in both air temperature measurement levels and they were distributed along the day as follows: (1) 0000–0500 UT, 111 samples; (2) 0500–0900 UT, 61 samples; (3) 0900–

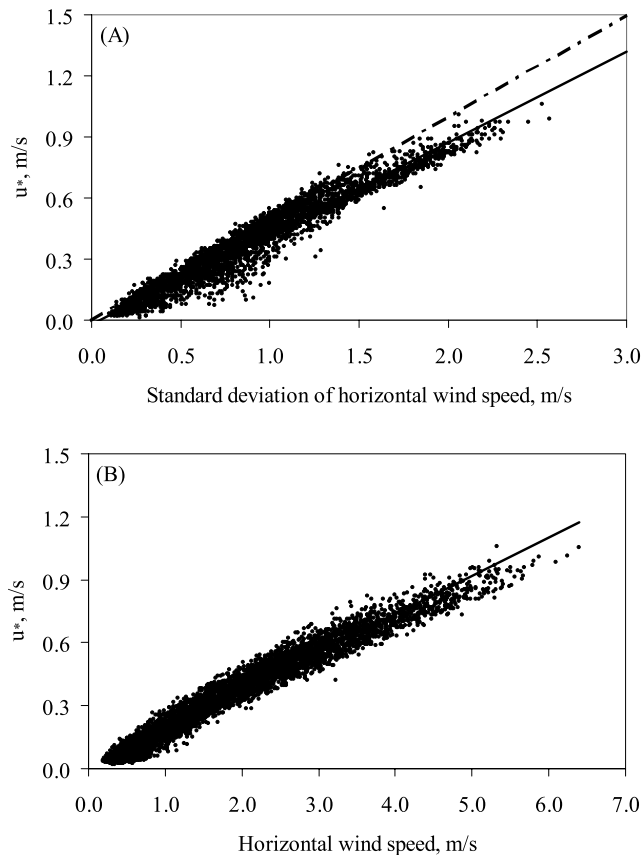


**Figure 2.** Actual friction velocity ( $u^*$ ) versus (a) the horizontal wind speed standard deviation (dashed line represents the 1:2 line introduced for comparing with the coefficient  $a_1 = 0.50$  found over homogeneous canopies [Kaimal and Finnigan, 1994]) and (b) the horizontal wind speed. In both cases the solid line represents the regression line.

1800 UT, 10 samples; (4) 1800–2200 UT, 52 samples; (5) 2200–2400 UT, 25 samples. This distribution corresponds to a total of 249 mistakes obtained under near neutral and stable conditions and 10 mistakes under slightly unstable conditions. The hourly intervals (bins) were selected to split the following periods: night, sunrise, daylight time including the typical capping inversion formation in the late afternoon, and sunset. It was found that during sunrise and sunset the lower level measurements (3.5 m) showed more mistakes (24 samples) than the upper level (5.1 m). For comparison, the performance of the method proposed by Wesson *et al.* [2001] for distinguishing

atmospheric surface layer stability conditions was also analyzed; unstable conditions were assumed when the available net surface energy was positive and vice versa. It was assumed that the energy storage below the net radiometer could be neglected (the canopy was open, without understories and the crown was not very dense). Then, with the Wesson *et al.* [2001] method, unstable and stable conditions were assumed when net radiation minus soil heat flux ( $Rn-G$ ) was positive and negative, respectively. This procedure led to 250 mistakes with similar hourly distribution to the previously mentioned. Therefore, in general, both procedures showed a similar performance. This set of 259 samples was discarded so as not to distort the aim of this paper. Further analysis was therefore carried out on a set of 3534 samples; 1898 samples gathered under unstable conditions and 1636 under stable conditions.

[21] Figures 2a and 2b show the actual friction velocity versus the standard deviation of horizontal wind speed and the mean wind speed, respectively, for all the data. Figure 2 indicates that equations (10a) and (10b) performed well in the roughness sublayer for our heterogeneous canopy. Table 1 lists the results obtained from simple linear regression analysis for equations (10a) and (10b) for all the data, unstable and stable conditions.

[22] The bias (coefficient  $b_0$  in Table 1) can, in practice, be neglected because the main influence of the friction velocity in estimating the sensible heat flux is under stable conditions. Whatever the expression used, the regression slopes obtained (coefficient  $b_1$ , Table 1) appeared robust. For equation (10a) the slope was close to  $a_1 = 0.50$  found over homogeneous canopies [Kaimal and Finnigan, 1994]. For equation (10b) the results were also good, though the coefficient  $a_2$  was lower than typical values obtained over uniform canopies [Kaimal and Finnigan, 1994; Raupach *et al.*, 1996] indicating that less momentum is absorbed due to the free space between trees and because olives trees have not a such dense crown in comparison with other studied canopies.

[23] A sonic anemometer was the only type of anemometer available during the experiment. Then, a lower accuracy than that shown in Figure 2 and Table 1 for equation (10a) will be obtained in practice because low-budget anemometers have lower time response to wind fluctuations. However, affordable anemometers measure the mean wind speed accurately. Therefore equation (10b) may then suit better our purposes than equation (10a) because it allows to bypass the instrumental error associated to low time response of the anemometer.

[24] Figure 3 shows the performance of equation (9) for all the data gathered from the sonic anemometer. It is interesting to outline the good performance obtained under

**Table 1.** Simple Linear Regression Analysis for Equations (10a) and (10b)<sup>a</sup>

Data Set	Equation (10a): $u^* = b_1 \sigma_u + b_0$			Equation (10b): $u^* = b_1 u + b_0$		
	$R^2$	$b_0$ , m/s	$b_1$	$R^2$	$b_0$ , m/s	$b_1$
All data	0.94	−0.02	0.45	0.95	0.01	0.18
Unstable conditions	0.93	−0.02	0.45	0.94	0.04	0.175
Stable conditions	0.96	−0.01	0.45	0.96	−0.01	0.18

<sup>a</sup> $R^2$ , coefficient of determination;  $b_0$ , intercept (bias);  $b_1$ , regression slope.

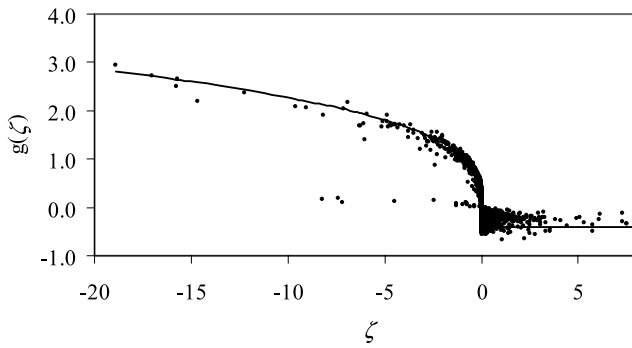


**Figure 3.** Performance of equation (9): stability function [ $g(\zeta)$ ] versus the stability parameter ( $\zeta$ ) corresponding to 1.4 m above the canopy top.

unstable conditions for such heterogeneous canopy and with constants  $C_0 = 0.05$  and  $C_1 = 0.95$ . After removing 16 samples that clearly were spurious data (see Figure 3) the following coefficients were obtained for the simple linear regression between  $g(\zeta)$  and  $\sigma_T/T^*$ : slope, 0.99; bias, 0.035; and  $R^2 = 0.94$ . Figure 3 confirms that the assumption of negligible zero plane displacement was appropriate. Under stable conditions the scatter was considerable for  $0 < \zeta < 3$ . A rapid convergence to the  $z$ -less relationship was not found indicating that MOST failed in such conditions. For this type of sparse tall vegetation, spatial temperature differences close to the canopy are expected to be large during nighttime. Cool air formed by radiative cooling at the top of the sparse vegetation would be mixed in a patchy way with underlying warmer air due to buoyancy. These local temperature variations do not contribute for the entire vertical flux of heat in the surface layer above the canopy. Therefore, when observations close to the canopy are used, one may expect a violation of the FV method. For this reason, this method was not used for describing flux predictions under stable conditions.

[25] Tables 2 and 3 list the simple regression analyses of estimated (dependent variable  $y$ ) sensible heat flux ( $H$ ) using the SR analysis and the FV methods versus that measured using the eddy covariance method (independent variable  $x$ ). In Table 2, estimates of  $H$  were determined using three different values for the friction velocity: (1)

measured by the sonic anemometer, (2) estimated as  $u_* = 0.45 \sigma_u$  (equation (10a)), and (3) estimated as  $u_* = 0.18 u$  (equation (10b)). These comparisons were made for all the data, unstable conditions, and stable conditions. Table 3 shows the performance for the free convection limit approaches, equations (6) and (8).

[26] Under unstable conditions, Table 2 indicates that the performance obtained using SR analysis, equation (5), and the FV method, equation (7), was good in general. SR analysis showed an excellent performance for the upper measurement height with a root mean square error (RMSE) value within a typical error for the eddy covariance. The mean air temperature during the campaign was  $25^\circ\text{C}$  under unstable conditions. Mean vertical velocities of about  $10^{-3}$  m/s are not detectable by eddy correlation systems [Mortensen, 1994]. Therefore, assuming a mean vertical velocity of  $10^{-3}$  m/s and air temperatures close to  $20^\circ\text{C}$ , a missing convective transport for sensible heat flux ( $H = \rho C_p \bar{w} \bar{T}$ ) close to  $24 \text{ W/m}^2$  should be expected. This figure is a realistic measurement error when measuring sensible heat flux using the eddy covariance technique under unstable conditions.

[27] Whatever the measurement height, equation (5) led to lower bias and higher determination coefficient than equation (7) mainly because the FV method was not as accurate for low values of sensible heat flux as SR analysis. Such performance is shown in Figure 4 for the upper measurement level. Figure 4 compares the estimates obtained from equations (5) and (7) ( $H_{SR-UP}$  and  $H_{FV-UP}$  respectively) versus the measured using the eddy covariance under unstable conditions. Similar performance was obtained for the lower measurement level. For equation (7) a lower RMSE value was obtained for the low measurement height than that for the upper measurement level (Table 2). This cannot be attributed to a better performance of the flux variance method when measuring at the canopy top. According to Högström [1990] this was as a consequence that the FV method was uncertain near neutral conditions (Figure 4).

[28] For equations (6) and (8), whatever the measurement level, Table 3 shows that SR analysis performed slightly better than the FV method. Estimates of  $H$  obtained with these two equations showed a similar bias and regression slopes of that obtained with equations (5) and (7). However,

**Table 2.** Linear Fit Regression and Root-Mean-Square Errors of Sensible Heat Flux ( $H$ ) Estimated Using the SR Analysis and the FV Methods (Dependent Variables  $y$ ) Versus That Measured Using the Eddy Covariance Method (Independent Variable  $x$ )<sup>a</sup>

Data Set	Variable $y^b$	$R^2$			$b_0, \text{W/m}^2$			$b_1$			RMSE, $\text{W/m}^2$		
		$u_{*m}$	$u_{*10a}$	$u_{*10b}$	$u_{*m}$	$u_{*10a}$	$u_{*10b}$	$u_{*m}$	$u_{*10a}$	$u_{*10b}$	$u_{*m}$	$u_{*10a}$	$u_{*10b}$
All data <sup>c</sup>	$H_{SR-UP}$	0.98	0.97	0.97	0.1	-0.8	-1.8	0.95	0.94	0.95	17.4	18.9	19.1
All data <sup>c</sup>	$H_{SR-LOW}$	0.98	0.97	0.97	0.3	1.3	0.0	1.15	1.14	1.14	19.3	28.6	28.7
Stable conditions <sup>c</sup>	$H_{SR-UP}$	0.83	0.82	0.71	2.1	1.8	-2.2	1.08	1.11	1.00	7.0	7.7	9.2
Stable conditions <sup>c</sup>	$H_{SR-LOW}$	0.85	0.84	0.71	1.1	0.7	-3.8	1.10	1.23	1.10	8.9	9.8	10.4
Unstable conditions	$H_{SR-UP}$	0.93	0.92	0.92	5.0	5.7	5.1	0.92	0.91	0.91	23.4	24.7	24.5
Unstable conditions	$H_{SR-LOW}$	0.93	0.91	0.91	10.1	13.3	11.2	1.04	1.08	1.08	35.2	38.0	37.4
Unstable conditions	$H_{FV-UP}$	0.90	0.86	0.84	25.7	29.6	29.3	1.02	1.00	0.98	39.7	45.2	43.8
Unstable conditions	$H_{FV-LOW}$	0.90	0.87	0.74	25.1	28.6	28.5	0.90	0.86	0.82	26.4	31.2	32.7

<sup>a</sup>Estimates of  $H$  obtained using three different friction velocity values: (1) measured ( $u_{*m}$ ), (2) determined from equation (10a) ( $u_{*10a}$ ), and (3) determined from equation (10b) ( $u_{*10b}$ ).  $R^2$ , coefficient of determination;  $b_0$ , intercept (bias);  $b_1$ , regression slope.

<sup>b</sup>Subindices refer to SR, surface renewal analysis; FV, flux variance method; UP, upper measurement height; LOW, lower measurement height.

<sup>c</sup>Stable cases for the flux variance method are not included, see text.

**Table 3.** Linear Fit Regression and Root-Mean-Square Errors of Sensible Heat Flux ( $H$ ) Estimated Using the SR Analysis and the FV Methods (Dependent Variables  $y$ ) for the Free Convection Limit Case (Equations (6) and (8)) Versus That Measured Using the Eddy Covariance Method (Independent Variable  $x$ )<sup>a</sup>

Variable $y^b$	$R^2$	$b_0$ , $W/m^2$	$b_1$	RMSE, $W/m^2$
$H_{SR-FL-UP}$	0.87	2.9	0.92	31.0
$H_{SR-FL-LOW}$	0.85	10.8	1.04	39.8
$H_{FV-FL-UP}$	0.73	11.1	0.90	46.6
$H_{FV-FL-LOW}$	0.73	9.0	0.73	53.1

<sup>a</sup> $R^2$ , coefficient of determination;  $b_0$ , intercept (bias);  $b_1$ , regression slope.

<sup>b</sup>Subindices refer to SR, surface renewal analysis; FV, flux variance method; UP, upper measurement height; LOW, lower measurement height; FL, free convection limit.

the  $R^2$  and RMSE values were better for the estimates obtained with these last two equations. In general, estimates obtained with equations (5) and (6) were closer among them than those obtained with equations (7) and (8). Differences between (7) and (8) were higher for the lower than for the upper measurement height. Thus RMSE value increased from about  $30.0 W/m^2$  for  $H_{FV-LOW}$  (Table 2) to  $53.1 W/m^2$  for  $H_{VA-FL-LOW}$  (Table 3).

[29] Under stable conditions, equation (5) showed a good performance. Though it overestimated the actual sensible heat flux about 11%, SR analysis was unbiased, well correlated and showed relatively low RMSE values (Table 2). Figure 5 shows the estimates obtained from equation (5) for the upper measurement level versus the eddy covariance measured sensible heat flux under stable conditions. Though not shown, similar performance was

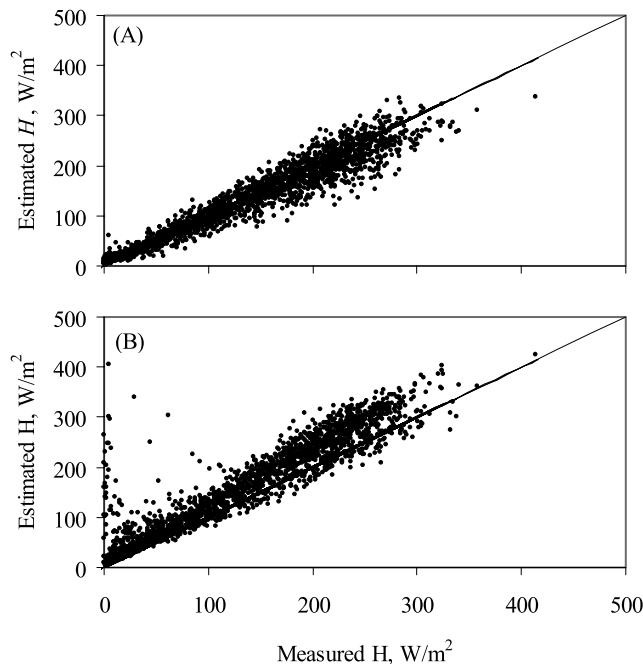


**Figure 4.** Performance of equations (5) and (7) under unstable conditions at the upper measurement height. Sensible heat flux ( $H$ ) estimates were obtained by (a) SR analysis ( $H_{SR-UP}$ ) and (b) the flux variance method ( $H_{VA-UP}$ ) versus measured (eddy covariance,  $H_{EC}$ ) sensible heat flux.

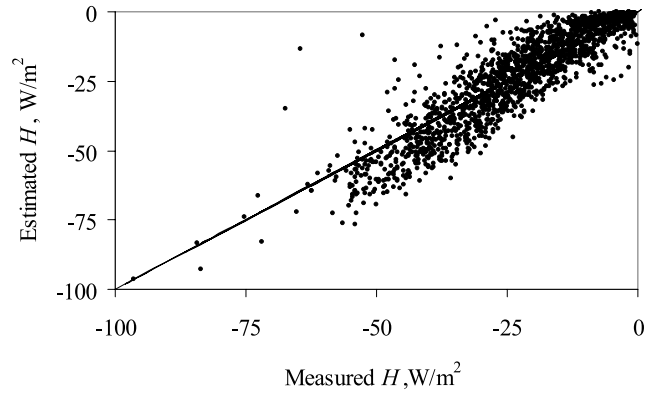


**Figure 5.** Performance of equation (5) under stable conditions at the upper measurement height.

obtained for the lower measurement height. For all the data set, SR analysis did good performance.

[30] If  $H$  estimates obtained using the actual friction velocity (Table 2) are taken as a reference for comparison, Table 2 shows that (1) whatever the procedure used for estimating the friction velocity, the SR analysis  $H$  estimates were comparable to the reference either for stable and unstable conditions and (2) similar results were also obtained for the flux variance method under unstable conditions. Then, the possible different bias introduced by equations (10a) or (10b), under determined atmospheric conditions, had a minor effect on the general performance. Consequently, since both equations (10a) or (10b) provided good estimates, equation (10b) fits better our objectives than equation (10a).

[31] SR analysis provided accurate sensible heat flux estimates because of the general good performance of equation (2) for estimating the  $\alpha$  parameter, whatever the stability conditions. Figure 6 shows the  $\alpha$  parameter estimates, equation (2), versus the actual half hourly values determined rearranging terms in equation (1) using the sensible heat flux measured with the sonic anemometer under unstable and stable conditions for the upper level as an example. Measurements taken at a single level were assumed, thus as mentioned above, the roughness sublayer height was estimated as a rule of thumb to a fixed height. However, Figure 6 shows that, in general, the  $\alpha$  parameter estimates were good for most of the samples. Then, a reliable representative value for the roughness sublayer height was chosen. It is interesting to note the square root dependence of the roughness sublayer height in equation (2); the  $\alpha$  parameter is therefore rather robust respect to moderate variations around a fixed roughness sublayer height. For correcting the vertical temperature gradient from the bottom to the top of the volume of air parcel to be renewed, Paw U *et al.* [1995] proposed to fix the  $\alpha$  parameter to 0.5 when measuring temperature traces at the top of homogeneous tall canopies. Katul *et al.* [1996] showed that  $\alpha$  parameter over forest was close to 0.5 but clearly dependent on the stability conditions. Castellvi [2004] showed that equation (2) was able to explain such performances. Figure 6 shows that the actual  $\alpha$  parameter is far to be close to 0.5 when measuring near the canopy top. Note that the surface was heterogeneous, thereby, the ratio roughness sublayer height over measurement height was



considerable. Equation (2) indicates that parameter  $\alpha$  depends on measurement height, stability conditions and wind speed but also the canopy structure plays an important role when measuring close to the canopy top.

[32] Those samples where equation (2) showed poor performance (Figure 6) were mostly gathered near neutral conditions. As an example, to better illustrate the performance of equation (2), Figure 7 shows the time evolution corresponding to half hourly samples of  $(Rn-G)$ , the estimated and the actual  $\alpha$  parameter during three typical days of the campaign (17–19 May). Despite the large differences between the estimated and the actual  $\alpha$  parameter for some samples when  $(Rn-G)$  is close to 0, Figure 4 shows that they had a minor effect for estimating sensible heat flux because near neutral conditions ramps have low amplitudes and frequencies. This issue is crucial for explaining the better performance of SR analysis than the FV method under unstable conditions shown in Table 2. Similarly, the FV method provided in general accurate sensible heat flux estimates under unstable conditions because of the good performance of equation (9). Figure 4b shows that the FV method tends to overestimate the sensible heat flux when exceeds, let say, about  $150 \text{ W/m}^2$ . Because equation (9) did good performance, the trend found in Figure 4b may be attributed to other factors. Following Weaver [1990] and Vogt *et al.* [2003], equation (9) likely requires to be adjusted at different levels when measuring close to the canopy.

[33] One may expect horizontal variation of flux measurements taken above but close of a heterogeneous canopy. This was confirmed by Vogt *et al.* [2003] for an olive orchard including measurements within the canopy. This

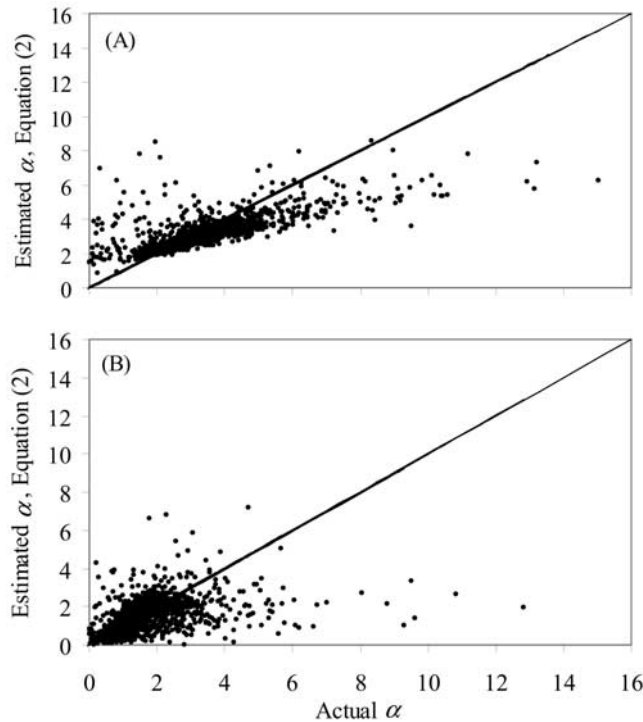


**Figure 6.** Performance of equation (2), showing estimated versus actual  $\alpha$  parameter at the upper measurement height for (a) unstable conditions and (b) stable conditions. Solid line represents the 1:1 line.

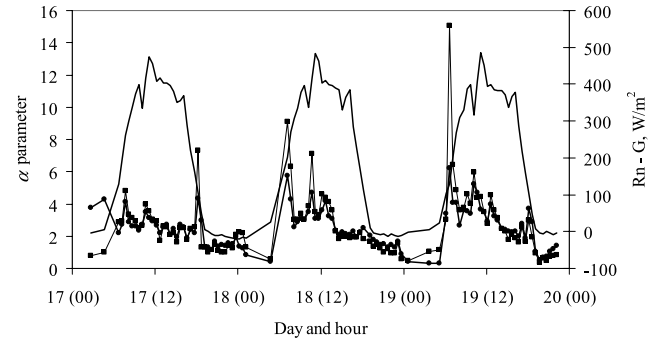


**Figure 7.** Time evolution of half hour  $(Rn-G)$  samples (solid line) and the estimated (equation (2), line with circles) and actual (line with squares)  $\alpha$  parameter values corresponding to the upper measurement height from 17 to 19 May.

indicates the need to average different local sensible heat flux measurements to provide a better assessment in  $H$ , such as we did for  $G$ , if one would escape fetch constraints and to set up a tall tower. Consequently, SR analysis in conjunction with equation (10b) suits the aim of this paper since it did good performance for different stability conditions and can be implemented using affordable instruments that permits a dense spatial cover.

## 5. Summary and Concluding Remarks

[34] This paper presents a long-term monitoring experiment for estimating sensible heat flux over a heterogeneous canopy where the total sensible heat flux comes from the canopy and the ground (olive orchard, 50% ground cover). For convenience, it was assumed that measurements of wind speed and air temperature were only available at a single level close to the canopy top. The performance for SR analysis and the FV method was evaluated. The SR analysis was found to be accurate, whatever the stability conditions. It was shown that a considerable dependence of the actual  $\alpha$  parameter was on the stability conditions and canopy structure (Figures 6 and 7). Thus SR analysis performed well because equation (2) provided, in general, good half-hourly estimates of the actual  $\alpha$  parameter. The performance of the FV method was good under unstable conditions and somehow uncertain near neutral conditions. Under stable conditions MOST failed. It is concluded that SR analysis was a robust method that was able to provide reliable sensible heat flux estimates over a heterogeneous canopy.

## Appendix A: Determination of the Ramp Parameters

[35] The two ramp models shown in Figure 1 provide similar results when determining ramp amplitude [Chen *et al.*, 1997a]. Then, structure functions (equation (A1)) and the analysis technique (equations (A2) to (A4)) from Van Atta [1977] were applied:

$$S^n(r) = \frac{1}{m-j} \sum_{i=1+j}^m (T_i - T_{i-j})^n \quad (\text{A1})$$



**Table A1.** Recommended Mean Values for  $\gamma$ ,  $r_x$ , and Sampling Frequencies for Different Canopies

Canopy and Height	$\gamma$	Frequency, Hz	$r_x$ , s
Fir forest (16.7 m)	1.001	5	0.833
Straw mulch (0.06 m)	1.175	11	0.111
Bare soil	1.104	26	0.066

where  $m$  is the number of data points in the 30-min interval measured at frequency ( $f$ ) in Hz,  $n$  is the power of the function,  $j$  is a sample lag between data points corresponding to a time lag ( $r = j/f$ ), and  $T_i$  is the  $i$ th temperature sample. An estimate of the mean value for the mean ramp amplitude  $A_T$  is determined by solving equation (A2) for the real roots:

$$A_T^3 + pA_T + q = 0 \quad (\text{A2})$$

where

$$p = 10S^2(r) - \frac{S^5(r)}{S^3(r)} \quad (\text{A3})$$

and

$$q = 10S^3(r) \quad (\text{A4})$$

[36] According to *Chen et al.* [1997a], the relationship between the inverse ramp frequency ( $\tau_T$ ) and ramp amplitude is

$$\frac{A_T}{\tau_T^{1/3}} = -\gamma \left[ \frac{S^3(r_x)}{r_x} \right]^{1/3} \quad (\text{A5})$$

where  $r_x$  is the time lag  $r$  that maximizes  $S^3(r)/r$  and  $\gamma$  is a parameter that corrects for the difference between  $A_T/\tau_T^{1/3}$  and the maximum value of  $[S^3(r)/r]^{1/3}$ . Parameter  $\gamma$  varies by less than 25% with respect to unity (0.9–1.2) for a range of canopies (Table A1). For bare soil and straw mulch, parameter  $\gamma$  mainly varies between 1.0 and 1.2, while for Douglas fir Forest it mainly varies between 0.9 and 1.1. Table A1 shows mean values for parameters  $\gamma$  and  $r_x$ , and suitable measurement frequencies (in Hz) for different canopies required to solve equation (A5), i.e., to find the appropriate solution for equation (A5) for the majority of samples [*Chen et al.*, 1997a, 1997b].

[37] **Acknowledgments.** The authors gratefully acknowledge K.T. Paw U and the reviewers for their valuable comments that substantially contributed to improving the paper. Thanks also go to Asun and Carla for her help in using various facilities at the University of Lleida and to Miguel Izquierdo, Jesús Gaudó, and Enrique Mayoral for field assistance. This work was supported under projects REN2001/CL11630 and CAO-01-AR-04 and grants from the Ministerio de Educación y Ciencia of Spain, Generalitat de Catalunya and the University of Lleida.

## References

- Albertson, J. D., M. B. Parlange, G. Katul, C. R. Chu, H. Striker, and S. Tyler (1995), Sensible heat flux estimates using variance methods, *Water Resour. Res.*, **31**(4), 969–974.
- Allen, R. G., W. O. Pruitt, J. A. Businger, L. J. Fritschen, M. E. Jensen, and F. H. Quinn (1996), Evaporation and transpiration, in *Hydrology*

- Handbook, ASCE Manual Rep. Eng. Pract.*, vol. 28, 2nd ed., edited by R. J. Heggen et al., pp. 125–252, Am. Soc. of Civ. Eng., Reston, Va.
- Brutsaert, W. (1988), *Evaporation into the atmosphere*, 299 pp., Springer, New York.
- Businger, J. A., J. C. Wyngaard, I. Izumi, and E. F. Bradley (1971), Flux profile relationships in the atmospheric surface layer, *J. Atmos. Sci.*, **28**, 181–189.
- Castellvi, F. (2004), Combining surface renewal analysis and similarity theory: A new approach for estimating sensible heat flux, *Water Resour. Res.*, **40**, W05201, doi:10.1029/2003WR002677.
- Castellvi, F., P. J. Perez, and M. Ibañez (2002), A method based on high-frequency temperature measurements to estimate the sensible heat flux avoiding the height dependence, *Water Resour. Res.*, **38**(6), 1084, doi:10.1029/2001WR000486.
- Cellier, P., and Y. Brunet (1992), Flux-gradient relationships above tall plant canopies, *Agric. For. Meteorol.*, **58**, 93–117.
- Chen, W., M. D. Novak, T. A. Black, and X. Lee (1997a), Coherent eddies and temperature structure functions for three contrasting surfaces. Part I: Ramp model with finite microfront time, *Boundary Layer Meteorol.*, **84**, 99–123.
- Chen, W., M. D. Novak, T. A. Black, and X. Lee (1997b), Coherent eddies and temperature structure functions for three contrasting surfaces. Part II: Renewal model for sensible heat flux, *Boundary Layer Meteorol.*, **84**, 125–147.
- De Bruin, H. A. R., N. J. Bink, and L. J. M. Kroon (1991), Fluxes in the surface layer under advective conditions, in *Land Surface Evaporation: Measurement and Parameterization*, edited by T. J. Schmugge and J. C. André, pp. 157–171, Springer, New York.
- De Bruin, H. A. R., W. Kohsiek, and B. J. J. M. Van Den Hurk (1993), A verification of some methods to determine the fluxes of momentum, sensible heat and water vapor using standard deviation and structure parameter of scalar meteorological quantities, *Boundary Layer Meteorol.*, **63**, 231–257.
- Goffe, W. L., G. D. Ferrier, and J. Rogers (1994), Global optimization of statistical functions with simulated annealing, *J. Econometrics*, **60**, 65–100.
- Högström, U. (1990), Analysis of turbulent structure in the surface layer with a modified similarity formulation of near neutral conditions, *J. Atmos. Sci.*, **47**, 1949–1972.
- Hsieh, C., and G. Katul (1996), Estimation of momentum and heat fluxes using dissipation and flux variance methods in the unstable surface layer, *Water Resour. Res.*, **32**(8), 2453–2462.
- Kader, B. A., and A. M. Yaglom (1990), Mean fields and fluctuation moments in unstably stratified turbulent boundary layers, *J. Fluid Mech.*, **212**, 637–662.
- Kaimal, J. C., and J. J. Finnigan (1994), *Atmospheric Boundary Layer Flows, Their Structure and Measurement*, 289 pp., Oxford Univ. Press, New York.
- Katul, G., M. Goltz, C. Hsieh, Y. Cheng, F. Mowry, and J. Sigmon (1995), Estimation of surface heat and momentum fluxes using the flux variance method above uniform and non-uniform terrain, *Boundary Layer Meteorol.*, **74**, 237–260.
- Katul, G., C. Hsieh, R. Oren, D. Ellsworth, and N. Philips (1996), Latent and sensible heat flux predictions from a uniform pine forest using surface renewal and flux variance methods, *Boundary Layer Meteorol.*, **80**, 249–282.
- Lloyd, C. R., A. D. Culf, A. J. Dolman, and J. H. C. Gash (1991), Estimates of heat flux from observations of temperature observations, *Boundary Layer Meteorol.*, **57**, 311–322.
- Metropolis, N., A. Rosenbluth, M. Rosenbluth, A. Teller, and E. Teller (1953), Equations of state calculations by fast computing machines, *J. Chem. Phys.*, **21**, 1087–1092.
- Mortensen, N. G. (1994), Wind measurements for wind energy applications, a review, in *Wind Energy Conversion 1994: Proceedings of the 16th British Wind Energy Association Conference, Stirling, June 15–17*, pp. 353–360, Br. Wind Energy Assoc., London.
- Padro, J. (1993), An investigation of flux variance methods and universal functions applied to three land-use types in unstable conditions, *Boundary Layer Meteorol.*, **66**, 413–425.
- Pahlow, M., M. B. Parlange, and F. Porté-Agel (2001), On Monin-Obukhov similarity in the stable atmospheric boundary layer, *Boundary Layer Meteorol.*, **99**, 225–248.
- Paw U, K. T. (2002), Coherent structures and surface renewal, in *Advanced Short Course on Agricultural, Forest and Micro Meteorology*, edited by F. Rosi, P. Duce, and D. Spano, pp. 63–76, Cons. Naz. delle Ric., Rome.

- Paw U, K. T., J. Qiu, H. B. Su, T. Watanabe, and Y. Brunet (1995), Surface renewal analysis: A new method to obtain scalar fluxes without velocity data, *Agric. For. Meteorol.*, **74**, 119–137.
- Press, W. H., S. A. Teukolsky, W. T. Vetterling, and B. P. Flannery (1992), *Numerical Recipes in C: The Art of Scientific Computing*, 2nd ed., 994 pp., Cambridge Univ. Press, New York.
- Raupach, M. R., J. J. Finnigan, and Y. Brunet (1996), Coherent eddies in vegetation canopies: The mixing layer analogy, *Boundary Layer Meteorol.*, **78**, 351–382.
- Snyder, R. L., D. Spano, and K. T. Paw U (1996), Surface renewal analysis for sensible and latent heat flux density, *Boundary Layer Meteorol.*, **77**, 249–266.
- Spano, D., R. L. Snyder, P. Duce, and K. T. Paw U (1997), Surface renewal analysis for sensible heat flux density using structure functions, *Agric. For. Meteorol.*, **86**, 259–271.
- Spano, D., R. L. Snyder, P. Duce, and K. T. Paw U (2000), Estimating sensible and latent heat flux densities from grapevine canopies using surface renewal, *Agric. For. Meteorol.*, **104**, 171–183.
- Stull, R. B. (1991), *An Introduction to Boundary Layer Meteorology*, 666 pp., Springer, New York.
- Tillman, J. E. (1972), The indirect determination of stability, heat and momentum fluxes in the atmospheric boundary layer from simple scalar variables during dry unstable conditions, *J. Appl. Meteorol.*, **11**, 783–792.
- Van Atta, C. W. (1977), Effect of coherent structures on structure functions of temperature in the atmospheric boundary layer, *Arch. Mech.*, **29**, 161–171.
- Vogt, R., A. Christen, and A. Pitacco (2003), Scintillometer measurements in a Cork oak and an olive tree plantation, paper presented at 5th Conference on Biometeorology, Ger. Meteorol. Soc., Dresden.
- Weaver, H. L. (1990), Temperature and humidity flux-variance relations determined by one-dimensional eddy correlation, *Boundary Layer Meteorol.*, **53**, 77–91.
- Wesely, M. (1988), Use of variance techniques to measure dry air-surface exchange rates, *Boundary Layer Meteorol.*, **44**, 13–31.
- Wesson, K. H., G. Katul, and C.-T. Lai (2001), Sensible heat flux estimation by flux variance and half-order time derivative methods, *Water Resour. Res.*, **37**(9), 2333–2343.
- Zapata, N., and A. Martínez-Cob (2001), Estimation of sensible and latent heat flux from natural sparse vegetation surfaces using surface renewal, *J. Hydrol.*, **254**, 215–228.

---

F. Castellvi, Departamento Medi Ambient i Ciències del Sòl, ETSEA, Rovira Roure 191, E-25198 Lleida, Spain. (f-castellvi@macs.udl.es)

A. Martínez-Cob, Departamento Genética y Producción Vegetal (EEAD), LAAMA (DGA-CSIC), Apartado 202, E-50080 Zaragoza, Spain. (macoan@eead.csic.es)